Available online at www.sciencedirect.com
ScienceDirect
Journal of Power Sources 179 (2008) 232–239
JOURNAL OF POWER SOURCES
www.elsevier.com/locate/jpowsour

Predictive control of SOFC based on a GA-RBF neural network model

Xiao-Juan Wu *, Xin-Jian Zhu, Guang-Yi Cao, Heng-Yong Tu

Institute of Fuel Cell, Department of Automation, Shanghai Jiao Tong University, Shanghai 200030, China

Received 7 December 2007; accepted 11 December 2007
Available online 23 December 2007

Abstract

Transients in a load have a significant impact on the performance and durability of a solid oxide fuel cell (SOFC) system. One of the main reasons is that the fuel utilization changes drastically due to the load change. Therefore, in order to guarantee the fuel utilization to operate within a safe range, a nonlinear model predictive control (MPC) method is proposed to control the stack terminal voltage as a proper constant in this paper. The nonlinear predictive controller is based on an improved radial basis function (RBF) neural network identification model. During the process of modeling, the genetic algorithm (GA) is used to optimize the parameters of RBF neural networks. And then a nonlinear predictive control algorithm is applied to track the voltage of the SOFC. Compared with the constant fuel utilization control method, the simulation results show that the nonlinear predictive control algorithm based on the GA-RBF model performs much better.

Keywords: Solid oxide fuel cell (SOFC); Fuel utilization; Load transient; Model predictive control (MPC)

1. Introduction

Compared to conventional heat engines, steam and gas turbine, and combined cycles, fuel cells are considered as an efficient electrical power generator. Among the various types of fuel cell, solid oxide fuel cell (SOFC) has attracted considerable interest as it offers wide application ranges, flexibility in the choice of fuel, high system efficiency and possibility of operation with an internal reformer [1].

Transients in a load have a significant impact on the life of the SOFC. One of the reasons is that the fuel utilization changes drastically due to the load transient. Fuel utilization u_f is one of the most important operating variables of the SOFC system. An overused-fuel condition ($u_f > 0.9$) could lead to permanent damage to the cells due to fuel starvation and an underused-fuel condition ($u_f < 0.7$) results in a rapid rise of the cell voltage [2]. For protecting the SOFC stack, the desired range of fuel utilization is from 0.7 to 0.9.

During the last decades, numerous dynamic models have been developed to study the effects of load transients on the performance and durability of the SOFC system [3–6]. These models include the electrochemical, thermal and mass flow aspects of fuel cell operation. Unfortunately, very few articles are available on the development of effective control strategies of the fuel utilization.

The terminal voltage and the fuel utilization cannot be kept constant simultaneously when load changes [7]. So there are two control strategies, which can guarantee the fuel utilization to operate within a safe range. One is directly controlling the input hydrogen fuel in proportion to the stack current, and the constant utilization control can be accomplished, which is analyzed in Ref. [8]. The other one is to maintain a constant cell voltage at the SOFC terminal. One proper value for cell voltage can guarantee the fuel utilization within the desired safe rang when the load changes.

In this paper, a nonlinear model predictive control (MPC) scheme is proposed to control the voltage and guarantee the fuel utilization within a safe range. The SOFC system is an uncertain nonlinear system and its structure and parameters vary with the change of operating point. So the controller should be robust to uncertainty and meet closed-loop objectives such as tracking, regulation and disturbance attenuation.

MPC is a feedback control strategy based on a predictive model and receding horizon optimization. The important advantage of MPC comes from the predictive model, which allows the design of controller in bigger horizon than the other control

* Corresponding author at: Institute of Fuel Cell, Shanghai Jiao Tong University, 800 Dongchuan Road, Minhang Campus, Shanghai 200030, China. Tel.: +86 21 34203657; fax: +86 21 62932154.
E-mail address: xj_wu@sjtu.edu.cn (X.-J. Wu).

0378-7753/$ – see front matter © 2007 Elsevier B.V. All rights reserved.
doi:10.1016/j.jpowsour.2007.12.036

Nomenclature

b_i	width of Gaussian membership function
c_i	center of Gaussian membership function
CV	conversion factor
E	open-circuit reversible potential (V)
E^0	standard reversible cell potential (V)
F	Faraday's constant (c mol^{-1})
I	stack current (A)
I_L	limiting current (A)
K_{H_2}	valve molar constants for hydrogen (mol s^{-1} Pa)
K_{H_2O}	valve molar constants for water (mol s^{-1} Pa)
K_{O_2}	valve molar constants for oxygen (mol s^{-1} Pa)
K_r	constant
n	number of electrons participating in the reaction
N	number of cells in the stack
p_{H_2}	partial pressure of hydrogen (atm)
p_{H_2O}	partial pressure of water (atm)
p_{O_2}	partial pressure of oxygen (atm)
P	cell pressure (atm)
P_{dc}	rated power (kW)
q_f	nature gas flow rate(mol s^{-1})
$q_{H_2}^{in}$	input hydrogen flow (mol s^{-1})
$q_{H_2}^{o}$	output hydrogen flow (mol s^{-1})
$q_{H_2}^{r}$	hydrogen flow that reacts (mol s^{-1})
q_i^{in}	input flow (mol s^{-1})
q_i^{o}	output flow (mol s^{-1})
q_i^{r}	flow that reacts (mol s^{-1})
$q_{O_2}^{in}$	input oxygen flow (mol s^{-1})
r_{H-O}	hydrogen–oxygen flow ratio
R	gas constant (J mol^{-1} K)
R_{Ohmic}	Ohmic resistance (Ω)
T	cell temperature (K)
u_i	membership function
u_f	fuel utilization
U	output voltage (V)
U_r	rated voltage (V)
V	compartment volume (m^3)

Greek symbols

α	electron transfer coefficient at the electrode
β	Tafel slope
η_{act}	activation losses (V)
η_{conc}	concentration loss (V)
η_{Ohmic}	Ohmic losses (V)
τ_{H_2}	response time for hydrogen flow (s)
τ_{H_2o}	response time for water flow (s)
τ_{O_2}	response time for oxygen flow (s)
τ_1	reformer time constants (s)
∂	Tafel constant

algorithms without the form of predictive model [9]. Therefore, the model is the key to determine the control quality. The traditional approach usually is based on approximate linearization theory, which is often difficult to identify an accurate mathematical model of the system and imposes serious restrictions on the structure of nonlinear systems [10]. Moreover, the robustness of the closed-loop system cannot be guaranteed, especially when the parameters of plant are uncertain or there is noise or disturbance in the process [11]. Therefore specific nonlinear modeling approaches might be required. Neural networks are considered as an attractive structure to establish the mathematical relationship of the dynamic system based on the input–output data. A RBF neural network is a feedforward neural network with one hidden layer and can uniformly approximate any continuous function to a prospected accuracy [12]. However, a key problem by using the RBF neural network approach is about how to choose the optimum initial values of the following three parameters: the output weights, the centers and widths of the hidden unit. If they are not appropriately chosen, the RBF neural network may degrade validity and accuracy of modeling [13]. To assure the optimal performance of the RBF neural network approach for SOFC modeling, we consider applying a genetic algorithm (GA) to optimize the RBF neural network parameters in this study. Genetic algorithms are a kind of self-adaptive global searching optimization algorithm based on the mechanics of natural selection and natural genetic [14]. Different from conventional optimization algorithms, genetic algorithms are based on population, in which each individual is evolved parallel, and the ultimate result is included in the last population. In this paper, a physical model of a 100 kW SOFC system is used to generate the data required for the training and predicting of the GA-RBF model.

This paper is organized into six sections. Section 2 briefly describes the SOFC system. A dynamic SOFC mathematical model is built in Section 3. In Section 4 a nonlinear predictive control algorithm based on a GA-BRF model is explained in detail. In addition the constant fuel utilization method is also analyzed. Section 5 shows the results obtained with the two control algorithms. The last section concludes the paper by analyzing the obtained results.

2. SOFC system description

The SOFC system includes a fuel processing unit or the reformer and a fuel cell stack. Hydrogen is a main fuel for most type of fuel cells. Nevertheless, other fuels such as methane, methanol, ethanol, gasoline and oil derivatives can also be used when a reformer is included in a fuel cell system for converting the fuel to hydrogen.

The basic components of the SOFC are anode, cathode and two ceramic electrodes. In the fuel cell, fuel is supplied to the anode and air is supplied to the cathode. At the cathode–electrolyte interface, oxygen molecules accept electrons coming from the external circuit to form oxide ions. The electrolyte layer allows only oxide ions to pass through and at the anode–electrolyte interface, hydrogen molecules present in the fuel react with oxide ions to form steam and electrons get released. These electrons pass through the external circuit and reach the cathode–electrolyte layer, and thus the circuit is closed

[15]. The electrochemical reactions are given as follows:

$$\text{Anode side}: \quad H_2 + O^{2-} \rightarrow H_2O + 2e^- \tag{1}$$

$$\text{Cathode side}: \quad 1/2O_2 + 2e^- \rightarrow O^{2-} \tag{2}$$

$$\text{Balance reaction}: \quad H_2 + 1/2O_2 \rightarrow H_2O \tag{3}$$

A single cell produces an open-circuit voltage of approximately 1 V, so fuel cells have to be connected together in a series arrangement to form a stack.

Fuel utilization is one of the most important operating variables that may affect the performance of fuel cell. It is defined as

$$u_f = \frac{q_{H_2}^{in} - q_{H_2}^{o}}{q_{H_2}^{in}} = \frac{q_{H_2}^{r}}{q_{H_2}^{in}} = \frac{NI}{2Fq_{H_2}^{in}} \tag{4}$$

3. SOFC system dynamic model

3.1. Fuel processing unit model

In Ref. [16], the author introduced a simple model of a reformer that generates hydrogen through reforming methane. The model is a second-order transfer function. Ref. [7] shows that fuel process approximated by first-order transfer functions was suitable for simulation point of view. So the mathematical form of the model can be written as follows:

$$\frac{q_{H_2}^{in}}{q_f} = \frac{CV}{\tau_1 s + 1} \tag{5}$$

When these reactants are fed into the SOFC stack where the reaction described by Eq. (3) occurs, from which it is seen that full reaction ratio between hydrogen and oxygen is 2 to 1. In order to allow for oxygen to completely react with hydrogen and maintain the pressure difference between the anode and the cathode below a certain threshold value, excess oxygen is provided. And oxygen flow rate is determined using the hydrogen–oxygen flow ratio r_{H-O}.

3.2. SOFC stack model

3.2.1. Electrochemical model

The electrochemical oxidation of CO is not considered in our study, because data in the literature show that the electrochemical oxidation of hydrogen is faster than that of CO [17]. Hence, the Nernst voltage E is mainly dependent on the electrochemical reaction of H_2.

In terms of input and output flow rates and exit molarity, the ith component material balance for the fuel cell stack can be written [18,19]:

$$\frac{dp_i}{dt} = \frac{RT}{V}(q_i^{in} - q_i^{o} - q_i^{r}) \tag{6}$$

According to the basic electrochemical relationships, the mole flow that reacts q_i^r can be calculated as

$$q_i^r = \frac{NI}{2F} = 2K_r I \tag{7}$$

Replacing the mole flow that reacts by Eq. (7), we can get the following expression of the hydrogen partial pressure

$$\frac{d}{dt}p_{H_2} = \frac{RT}{V}(q_{H_2}^{in} - q_{H_2}^{o} - 2K_r I) \tag{8}$$

For orifice that is choked, it could be considered that the molar flow of any gas through the valve is proportional to its partial pressure inside the channel, according to the expression

$$\frac{q_{H_2}}{p_{H_2}} = K_{H_2} \tag{9}$$

Replacing the output flow by Eq. (9), applying the Laplace transformation to Eq. (8) and isolating the hydrogen partial pressure, yields the following expressions:

$$p_{H_2}(s) = \frac{1/K_{H_2}}{1 + \tau_{H_2} s}(q_{H_2}^{in} - 2K_r I) \tag{10}$$

where $\tau_{H_2} = \frac{V}{K_{H_2} RT}$

Similarly component balances for O_2 and H_2O lead to the following set of equations:

$$p_{O_2}(s) = \frac{1/K_{O_2}}{1 + \tau_{O_2} s}(q_{O_2}^{in} - K_r I) \tag{11}$$

$$p_{H_2O}(s) = 2K_r I \frac{1/K_{H_2O}}{1 + \tau_{H_2O} s} \tag{12}$$

3.2.2. Operating cell voltage

The actual cell potential is decreased from its ideal potential because of several types of irreversible losses, such as activation, concentration and Ohmic losses. The equation for polarization is shown as follows:

$$\eta_{act} = \partial + \beta \log I \tag{13}$$

$$\eta_{conc} = \frac{RT}{2F} \ln\left(1 - \frac{I}{I_L}\right) \tag{14}$$

$$\eta_{Ohmic} = I^2 R \tag{15}$$

Applying Nernst's equation and Ohm's law (taking into account Ohmic, concentration, and activation losses), the stack output voltage is represented as follows:

$$V_{dc} = E - \eta_{Ohmic} - \eta_{conc} - \eta_{act} \tag{16}$$

where $E = N\left(E^0 + \frac{RT}{2F} \ln \frac{p_{H_2} p_{O_2}^{1/2}}{p_{H_2O}}\right)$

The dynamic physical model replaces the real SOFC stack to generate the simulation data required for the identification of the GA-RBF model. The parameters of the SOFC system are given in Table 1. The data sources blocks developed in MATLAB is shown in Fig. 1.

4. SOFC control

4.1. Constant voltage control

The basic frame of the proposed model predictive controller for the SOFC system is shown in Fig. 2, where y_r is the refer-

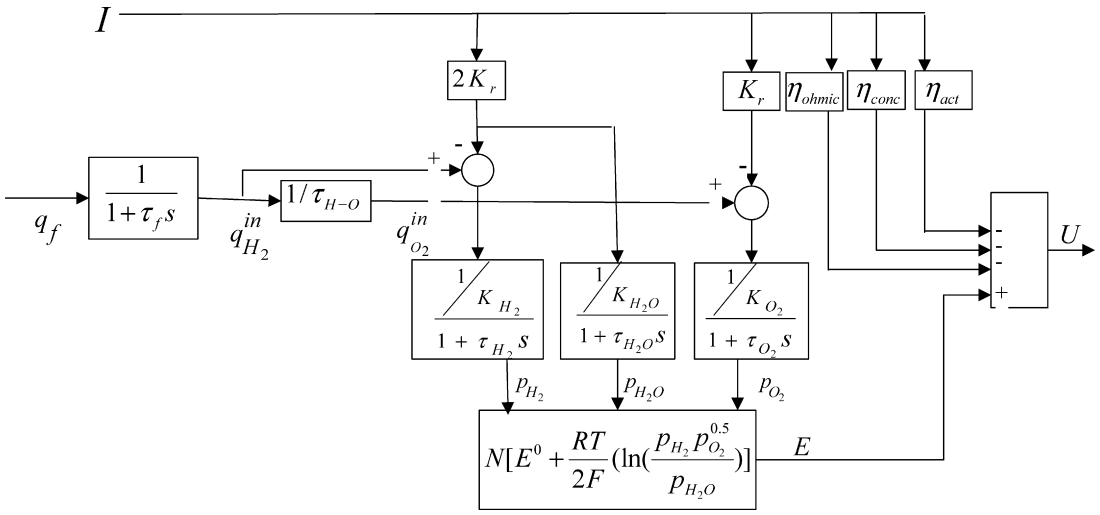

Fig. 1. SOFC dynamic model.

Table 1
The blocks developed in MATLAB

Parameter	Unit	Value
T	K	1273
F	C mol^{-1}	96485
R	J (mol K)$^{-1}$	8.314
N	–	384
E^0	V	1
K_r	mol (s A)$^{-1}$	0.996×10^{-3}
K_{H_2}	mol (s Pa)$^{-1}$	8.32×10^{-6}
K_{H_2O}	mol (s Pa)$^{-1}$	2.77×10^{-6}
K_{O_2}	mol (s Pa)$^{-1}$	2.49×10^{-5}
τ_{O_2}	s	2.91
τ_{H_2}	s	26.1
τ_{H_2O}	s	78.3
R_{Ohmic}	Ω	0.126
$q_{H_2}^{in}$	mol s^{-1}	Variable
β	–	0.11
∂	–	0.05
I_L	A	800
n	–	2
U	V	Variable
I	A	Variable
τ_1	s	5
r_{H-O}	–	1.145
CV	–	1
U_r	V	330
P_{dc}	kW	100
u_{fs}	–	0.8

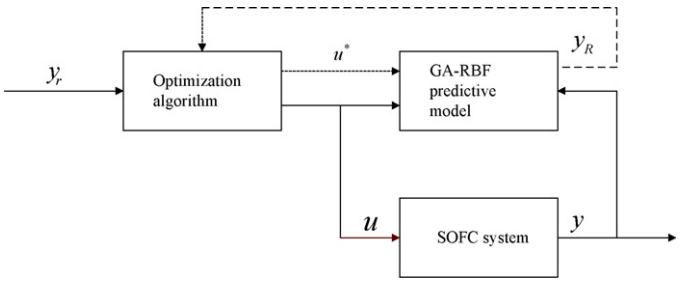

Fig. 2. Block diagram of the proposed control system.

ence track of the control system, y and y_R is the SOFC dynamic model output and the GA-RBF predictive model output, respectively.

A nonlinear model that the controller will use for the optimization is the first step in designing a nonlinear MPC system. This model should be as accurate as possible, while being simple enough to allow for repeated calculations during the optimization. If the dynamic model developed in Section 3 is applied in the predictive control scheme, it will consume much time to obtain the solutions. For this reason, a nonlinear offline voltage model of SOFC is built by a GA-RBF neural network.

4.1.1. Predictive model based on GA-RBF neural network

Suppose the operating temperature and pressure of the SOFC are kept constant in this paper. The oxygen flow is expressed by using the hydrogen–oxygen flow ratio, so the terminal voltage U is mainly influenced by the inlet hydrogen flow $q_{H_2}^{in}$ and current I. The following NARMAX model is used to describe the controlled voltage system

$$y(k) = f[y(k-1), y(k-2), \ldots, y(k-n_y), u(k-1), u(k-2), \ldots, u(k-n_u)] \quad (17)$$

where y is the SOFC terminal voltage, u is the hydrogen flow rate and current, n_y and n_u are the lags of the output and input, respectively, and $f(\cdot)$ is a nonlinear function. In this section we adopt a GA-RBF neural network to identify the nonlinear function $f(\cdot)$. The structure of the RBF neural network is shown in Fig. 3.

The output of hidden layer is

$$u_i = \exp\left[-\frac{(x-c_i)^T(x-c_i)}{2b_i^2}\right] \quad (i = 1, 2, \ldots, q) \quad (18)$$

where $x = (I,\ q_{H_2}^{in})^T$, $C_i = (c_{i1}, c_{i2})^T$ is the center of the ith RBF hidden unit, and b_i is the width of the ith RBF hidden unit.

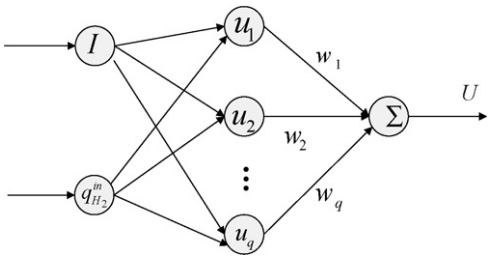

Fig. 3. The structure of the RBF neural network.

The output is

$$y_R = \sum_{i=1}^{q} w_i u_i \tag{19}$$

where $y_R = U$; $w = [w_1, w_2, \ldots w_q]^T$ is the neural network weight that connects output y_R and neuron i in the hidden layer.

In our case, it is done by minimizing the following quadratic cost function of the output error. This error is calculated by comparing the output value of the network and the desired output value.

$$J = \frac{1}{2}\sum_{k=1}^{M}[y_R(k) - y(k)]^2 \tag{20}$$

where y_R is the output voltage calculated from neural network; y the output voltage of the dynamic physical model developed in Section 3; M the number of training data. A gradient descent algorithm is adopted to minimize J. And the genetic algorithm is used to obtain the optimum initial values of the following three parameters: the output weight w_i, the centers c_i and widths b_i.

The predictive output of p step can be obtained by the GA-RBF model as [20]:

$$\begin{aligned} y_R(k+p) = f_R[&y(k+p-1), y(k+p-2), \ldots, \\ &y(k+p-n_y), u(k+p-1), u(k+p-2), \ldots, \\ &u(k+p-n_u)] \end{aligned} \tag{21}$$

And the error at instance k is defined as

$$e(k) = y(k) - y_R(k) \tag{22}$$

Therefore the predictive output of feedback system is

$$y(k+j) = y_R(k+j) + e(k) \quad (j = 1, 2, \ldots, p) \tag{23}$$

where p is the predictive horizon. The method of the offline model is simple and convenient only if the experimental data or experience of the input and output variable is obtainable. It is not necessary to decide the coefficient of the SOFC material and structure of the mechanism model. Therefore it can be used in the control system.

4.1.2. Optimization algorithm

At each sample time k, a series of future output values $y(k+j)$ is calculated through GA-RBF predictive model and it is compared to the reference output value $y_r(k)$. Referenced trajectories of output voltage are introduced to avoid excessive movement of the control input, which are defined as

$$y_r(k+j) = c^j y(k) + (1 - c^j) r \quad (1 \le j \le p,\ 0 < c < 1) \tag{24}$$

where y_r and y are the reference trajectories and predictive output, respectively. r is the system set value. The optimization problem for the model predictive controller is the minimization of the sum of squared errors between the referenced trajectory y_r and the predictive output y with an additional penalty imposed on rapid changes in the manipulated variables. Define objective function as

$$\begin{aligned} J(k) = &\sum_{j=1}^{n}[y_R(k+j) - y_r(k+j)]^2 + \sum_{j=1}^{m}\lambda u^2(k+i-1) \\ &u(k+i-1) \in U^* \end{aligned} \tag{25}$$

where n and m are the predictive horizon and control horizon, respectively. $U^* = [u_{min}, u_{max}]$ is the control range. Golden mean method is used to obtain the optimal output of controller $u^*(k)$, the optimization process is presented as follows [20]:

- Step 1: Define the initial searching area $[\alpha_1, \beta_1] = [u_{min}, u_{max}]$; the initial number of steps $k = 1$; and define ζ, it is positive and adequately small; the initial searching points are given as: $\lambda_1 = \alpha_1 + (1 - 0.618)(\beta_1 - \alpha_1)$, $\lambda_1' = \alpha_1 + 0.618(\beta_1 - \alpha_1)$. And then, compute the values of objective function $J(\lambda_1)$ and $J(\lambda_1')$.
- Step2: If $\beta_k - \alpha_k < \zeta$, then $u(k) = (\beta_k + \alpha_k)/2$; Otherwise, if $J(\lambda_k) > J(\lambda_k')$, go to step 3; if $J(\lambda_k) > J(\lambda_k')$, go to step 4.
- Step 3: $\alpha_{k+1} = \lambda_k$, $\beta_{k+1} = \beta_k$, $\lambda_{k+1} = \lambda_k'$, then $\lambda_{k+1}' = \alpha_{k+1} + 0.618(\beta_{k+1} - \alpha_{k+1})$; and then, compute the value of objective function $J(\lambda_{k+1}')$, go to Step 5.
- Step 4: $\alpha_{k+1} = \alpha_k$, $\beta_{k+1} = \lambda_k'$, $\lambda_{k+1}' = \lambda_k$, then $\lambda_{k+1} = \alpha_{k+1} + (1 - 0.618)(\beta_{k+1} - \alpha_{k+1})$; and then, compute the value of objective function $J(\lambda_{k+1})$; go to Step 5.
- Step 5: $k = K + 1$, return to Step 2.

After iterations for several times, the optimal control moves $u^*(k)$ can be obtained.

4.2. Constant fuel utilization control

According to Eq. (4), the operation of the SOFC stack with a fuel input proportional to the stack current results in a constant utilization factor in the steady-state. Thus, the SOFC is operated with a constant steady-state utilization factor by controlling the natural gas flow to the stack as [8]

$$q_f = \frac{NI}{2Fu_{fs}} \tag{26}$$

where u_{fs} is the desired utilization in steady-state. Furthermore, because the fuel processor is specially considered, the relationship between a small change of stack current ΔI and a small

change of hydrogen input in $\Delta q_{H_2}^{in}$ fed to the SOFC stack can be derived as [8]:

$$\Delta q_{H_2}^{in} = \frac{N}{2Fu_{fs}(1+\tau_f s)}\Delta I = \frac{2K_r}{u_{fs}(1+\tau_f s)}\Delta I \quad (27)$$

From Eq. (4), the small-signal relationship between Δu_f, ΔI, and $\Delta q_{H_2}^{in}$ about their initial steady-state values u_{fs}, I_0, and $q_{H_2,0}^{in}$ can be written as

$$\Delta I = \frac{q_{H_2,0}^{in}}{2K_r}\Delta u_f + \frac{u_{fs}}{2K_r}\Delta q_{H_2}^{in} \quad (28)$$

Under constant u_f control, substituting Eq. (27) into Eq. (28), and Eq. (28) can be rewritten as

$$\Delta u_f = \frac{u_{fs}}{I_0}\frac{\tau_f s}{1+\tau_f s}\Delta I \quad (29)$$

where I_0 the initial stack current, is related to the initial $q_{H_2,0}^{in}$ through Eq. (4).

5. Simulation

In this section, we present numerical experiments to show the validation of the proposed nonlinear predictive control scheme based on the GA-RBF neural network model of the SOFC.

For the purpose of identification, the input signals of the dynamic physical model developed in Section 3 are uniformly random, including the hydrogen flow rate (0–1.2 mol s^{-1}) and the current (0–800 A). To obtain values at integer time points, the fourth-order Runge–Kutta method was used to find the numerical solution to the dynamic physical model in the simulation. A set of 3000 data was collected from the simulation. The first 1000 data were used for the identification of GA-RBF model, while the remaining 2000 data were used for validation purposes.

In order to reduce the numbers of the parameters and improve the speed of program debug, the hidden layer of the RBF neural network is chosen 2 nodes. After many trials, a population size of 50, a crossover probability of 0.4, and a mutation probability of 0.001 are used. The optimized initial values of the parameters are shown in Table 2. After the optimized initial values of the three parameters are obtained, we utilize the gradient descent learning algorithms to adjust them. Root mean square error (RMSE) is employed here to evaluate modeling results, which is calculated

Table 2
The optimized initial values of widths, centers and output weights

b_1	0.4856
b_2	1.1062
c_{11}	0.5678
c_{12}	−0.3561
c_{21}	−0.8409
c_{22}	1.032
w_1	0.4567
w_2	−0.2365

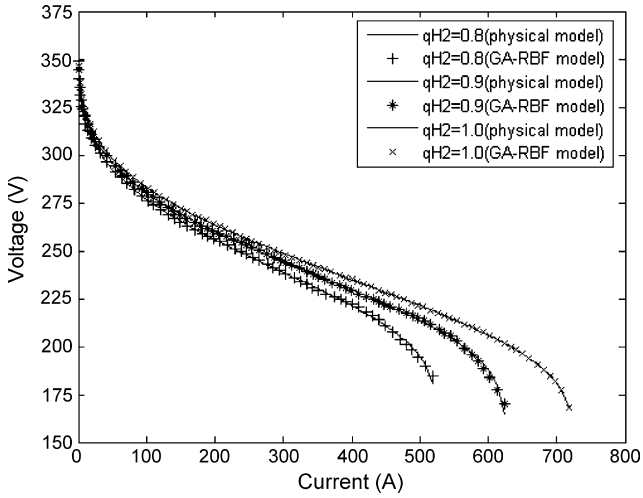

Fig. 4. Cell terminal voltage under various current and hydrogen flow.

by

$$\mathrm{RMSE} = \sqrt{\frac{1}{N}\sum_{k=1}^{N}(y(k)-\hat{y}(k))^2} \quad (30)$$

where N is the number of sample data from the dynamic physical model of SOFC, $y(k)$ is the predictive output of GA-RBF model, $\hat{y}(k)$ is the output of the dynamic physical model. Under various hydrogen flows and current, the voltage identification model is shown in Fig. 4. The RMSE of output voltage obtained is 1.2584 and 1.1836, respectively. The result shows that the GA-RBF neural network can approximate the behavior of the physical SOFC model with good accuracy.. The control input is shown in Fig. 7

In normal working condition, the current of the SOFC system is 300 A. The steady output of the voltage is 330 V. Assuming at $t = 200$ s, a load disturbance causes the stack current to have a step change (from 300 to 255 A), and at $t = 550$ s, a load disturbance causes the stack current to have a step change (from 255 to 345 A). The series of step in stack current input are shown in Fig. 5. The predictive controller is used to adjust the voltage to its steady value. In this paper, let the predictive horizon be

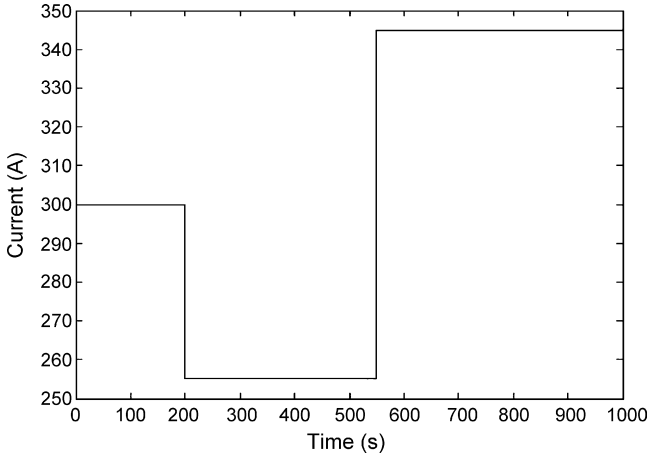

Fig. 5. Step increase in cell current.

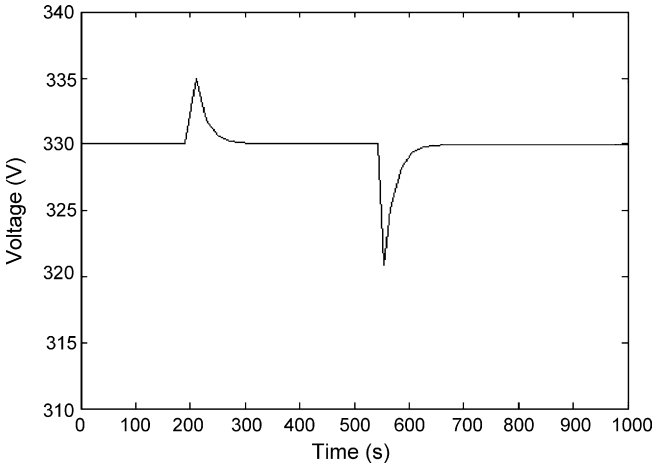

Fig. 6. Trajectories of SOFC voltage by MPC.

$m = 10$, and the control horizon $n = 4$. We can get the tracking curve of the controlled voltage of the SOFC system, which is shown in Fig. 6. From Fig. 6, we can get when the stack current fluctuates the voltage is changed rapidly and then returns to the reference value. Based on the results, we can get the fuel

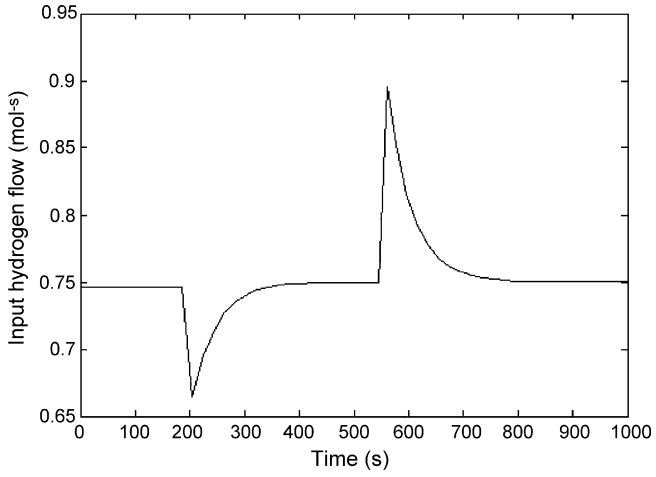

Fig. 7. Curves of manipulated variable $q_{H_2}^{in}$.

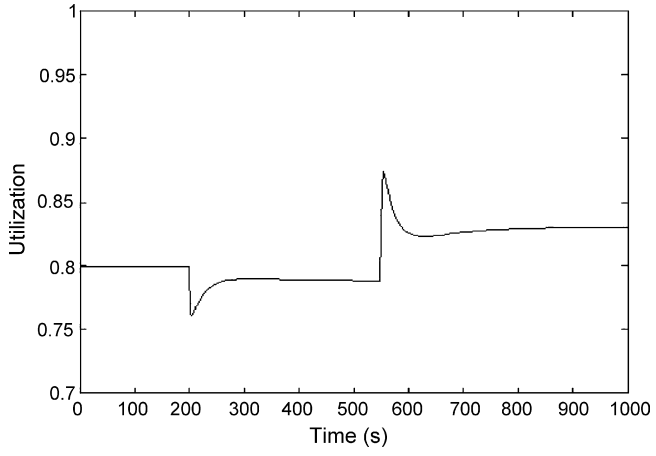

Fig. 8. Fuel utilization response by MPC.

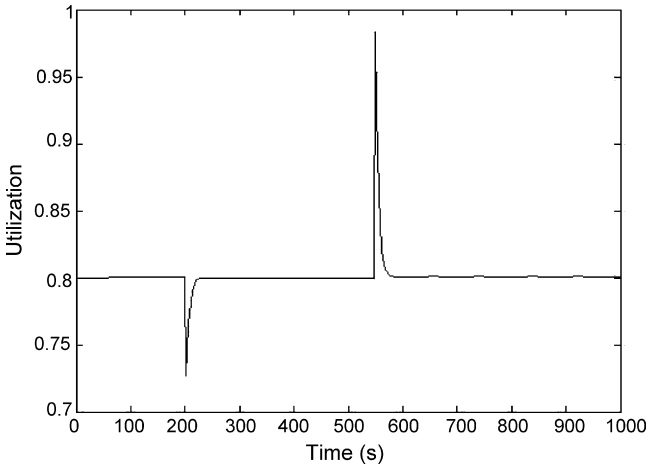

Fig. 9. Fuel utilization response by constant fuel utilization control.

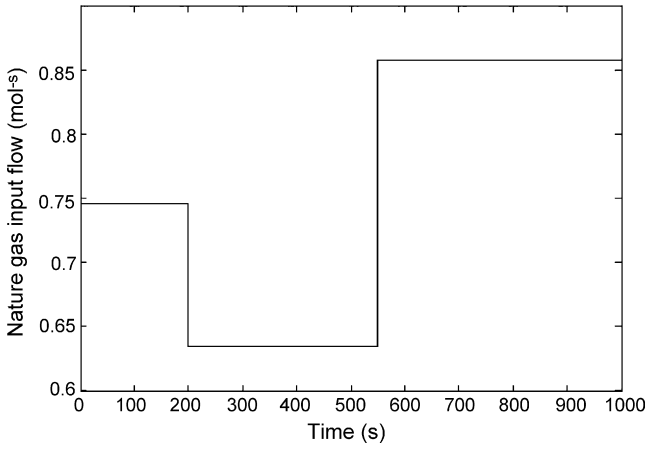

Fig. 10. Curves of manipulated variable q_f.

utilization response curve of the SOFC system, which is shown in Fig. 8. The result shows that the predictive control scheme can guarantee the fuel utilization of the SOFC operating within a safe range when load changes.

Now we use the same load disturbances as before and use the constant fuel utilization control method. The tracking curve of the controlled fuel utilization of the SOFC system is shown in Fig. 9. And the manipulated variable q_f is shown in Fig. 10. Comparing Fig. 8 with Fig. 9, we can get the conclusions: the constant fuel utilization control method is simpler; however the fuel utilization u_f has a larger excursion from the safe range when the stack current changes from 255 to 345 A at $t = 550$ s.

6. Conclusions

Fuel utilization is one of the most important controlled variables in the SOFC system. In order to guarantee the fuel utilization would operate within a safe range, a nonlinear predictive control algorithm based on a GA-RBF identification model is proposed to control the SOFC output voltage as a proper constant. By comparing the constant fuel utilization control method with the nonlinear model predictive controller scheme, the simulation results show that the MPC is com-

plex, however, it guarantees the fuel utilization performs more safely.

Acknowledgment

This work is supported by National 863 Scientific Project Development Funds (No. 2006AA05Z148), PR China.

References

[1] W. Sangtongkitcharoen, S. Vivanpatarakij, N. Laosiripojana, et al., Chem. Eng. J. (2007).
[2] S. Kourosh, F. Ali, IEEE Trans. Energy Convers. 21 (1) (2006) 250–256.
[3] J. Padullés, G.W. Ault, J.R. McDonald, J. Power Sources 86 (2) (2000) 495–500.
[4] D.J. Hall, R.G. Colclaser, IEEE Trans. Energy Convers. 14 (1999) 749–753.
[5] A. Elmar, J. Power Sources 57 (1/2) (1995) 105–109.
[6] S. Kourosh, F. Ali, IEEE Trans. Energy Convers. 19 (2) (2004) 423–428.
[7] Y.H. Li, S.S. Choi, S. Rajkaruna, IEEE Trans. Energy Convers. 20 (2) (2005) 381–387.
[8] Y.H. Li, S. Rajakaruna, S.S. Choi, IEEE Trans. Energy Convers. 22 (2) (2007) 405–413.
[9] G. Wei, H. Min, Proceedings of the 2006 American Control Conference Minneapolis, MN, USA, June 14–16, 2006, pp. 1569–1574.
[10] T. Van Den Boom, M.A. Botto, J. Sá Da Costa, Int. J. Control 76 (18) (2003) 1783–1789.
[11] K. Hwang, S. Tan, M. Tsai, IEEE Trans. Syst. Man Cybern. B: Cybern. 33 (3) (2003) 514–521.
[12] K. Warwick, Proceedings of the 35th Conference on Decision and Control, Kobe, Japan, December, 1996, pp. 464–469.
[13] X.-J. Wu, X.-J. Zhu, G.-Y. Cao, et al., J. Power Sources 167 (1) (2007) 145–150.
[14] D.E. Goldberg, Genetic Algorithms in Search, Optimization and Machine Learning, Addison-Wesley, 1989.
[15] J.R. Ferguson, J.M. Fiard, R. Herbin, J. Power Sources 58 (1) (1996) 109–122.
[16] M.Y. El-Sharkh, A. Rahman, M.S. Alam, A.A. Sakla, IEEE Trans. Power Syst. 19 (4) (2004) 2022–2028.
[17] P. Vernoux, J. Guindet, M. Kleitz, J. Electrochem. Soc. 145 (10) (1998) 3487–3492.
[18] J. Padulles, G.W. Ault, J.R. McDonanld, J. Power Sources 86 (2000) 495–500.
[19] K. Sedghisigarchi, A. Feliachi, IEEE Trans. Energy Convers. 19 (2) (2004) 423–428.
[20] J. Zhu, Intelligent Predictive Control Technology and Application [M], Zhejiang University Press, Hangzhou, 2006.